Study on the Preparation of PU/HBP-NH$_2$ Blend Film and Its Properties

Ren Longfang,[1] Wang Na,[1] Wang Xuechuan[1,2]

[1]Key Laboratory of Chemistry and Technology for Light Chemical Industry, Ministry of Education, Shaanxi University of Science and Technology, 710021 Shaanxi Xi'an, China

[2]Shaanxi Research Institute of Agricultural Products Processing Technology, Shaanxi University of Science and Technology, 710021 Shaanxi Xi'an, China

Correspondence to: R. Longfang (E-mail: renlf1010@163.com)

ABSTRACT: The blend films of polyurethane (PU) and amino-terminal hyperbranched polymers (HBP-NH$_2$) were prepared successfully by mixing HBP-NH$_2$ solution and PU. The rate of moisture absorption and mechanical properties were determined. The results showed that the rates of moisture absorption and vapor permeability were improved from 0.34% to 7.51% and from 161 gm^{-2} d^{-1} to 879 gm^{-2} d^{-1}, respectively. The addition of HBP-NH$_2$ is helpful to improve the hygiene properties of PU films. Then, the structures of the blend films were characterized by IR, XRD, TG, and SEM at the same time. The results indicated that HBP-NH$_2$ and PU had hydrogen-bond interaction and a certain phase separation. The blend films had good heat stability. © 2014 Wiley Periodicals, Inc. J. Appl. Polym. Sci. **2015**, *132*, 41383.

INTRODUCTION

Polyurethane (PU) is a kind of macromolecular compound, formed by the addition polymerization of diisocyanate or polyisocyanates with diols or polyols. It exhibits excellent properties, such as high strength, abrasion resistance, good low temperature resistance, chemical resistance, and good resilience. Therefore, it can be widely used in PU synthetic leather, leather finishing agent, and textile coating. However, PU film has poor moisture adsorption and vapor permeability, which directly influence the wearing comfort of product significantly.[1,2] Hyperbranched polymers are a type of dendrimers, which possess a large number of end groups. They have highly branched three-dimensional spherical structure and good qualities, such as no inter chain entangling, lower viscosity, and difficult to crystallization.[3–6] It was found that hyperbranched polymers were easily mixed with other polymers. As a result, it can be used as modifier in polymer materials.[7,8] Huber et al.[9] studied blends of hyperbranched poly (ether amide)s and polyamide-6 (PA6). They found that the glass transition temperature of blends increased with the increase of hyperbranched poly (ether amide)s, and it was bigger than its calculation value. This was because intermolecular hydrogen-bonding interaction was formed between the two components and the compatibility was better. The aromatic hyperbranched polyamide and PA6 blend modification were studied by Monticelli et al.[10] The compatibility of blend was better when 5% hyperbranched aramid were added, and the blend had only one T_g. In another study,[11] the

miscibility of PVDF and hyperbranched polyester (HBPE) was investigated using FTIR and DSC techniques. The results indicated that the materials are intimately mixed due to either relatively weak H-bonding and/or dipole–dipole interaction.

Blending is an effective and feasible method to improve the performance of polymer materials. The relationship between each component in the blending system is mainly physical interaction and has certain intermolecular forces. By combining the most desirable characteristics of each component, it is expected to obtain polymer blends with unique properties.[12] There are many studies on the blend films of silk fibroin, chitosan, and wool powder with PU.[13–16] Researchers hope to improve moisture absorption of the PU films by introducing those hydrophilic materials, and the results show that the modification effect is excellent. Compared with natural polymer, the addition of hyperbranched polymers can decrease the viscosity of the blend system due to their lower entanglement concentration. Moreover, it can also reduce emissions because of their higher solubility in solvents. In this article, the blend films of PU and amino-terminal hyperbranched polymers (HBP-NH$_2$) were prepared by mixing HBP-NH$_2$ solution and PU so as to improve the vapor permeability and moisture absorption of PU film, while other properties of film need to be maintained.

EXPERIMENTAL

Main Reagents and Instruments

Hyperbranched polymers were self-prepared. (HBP-NH$_2$, 50%). *N,N* dimethyl formamide (DMF), *N,N*-methylenebisacrylamide
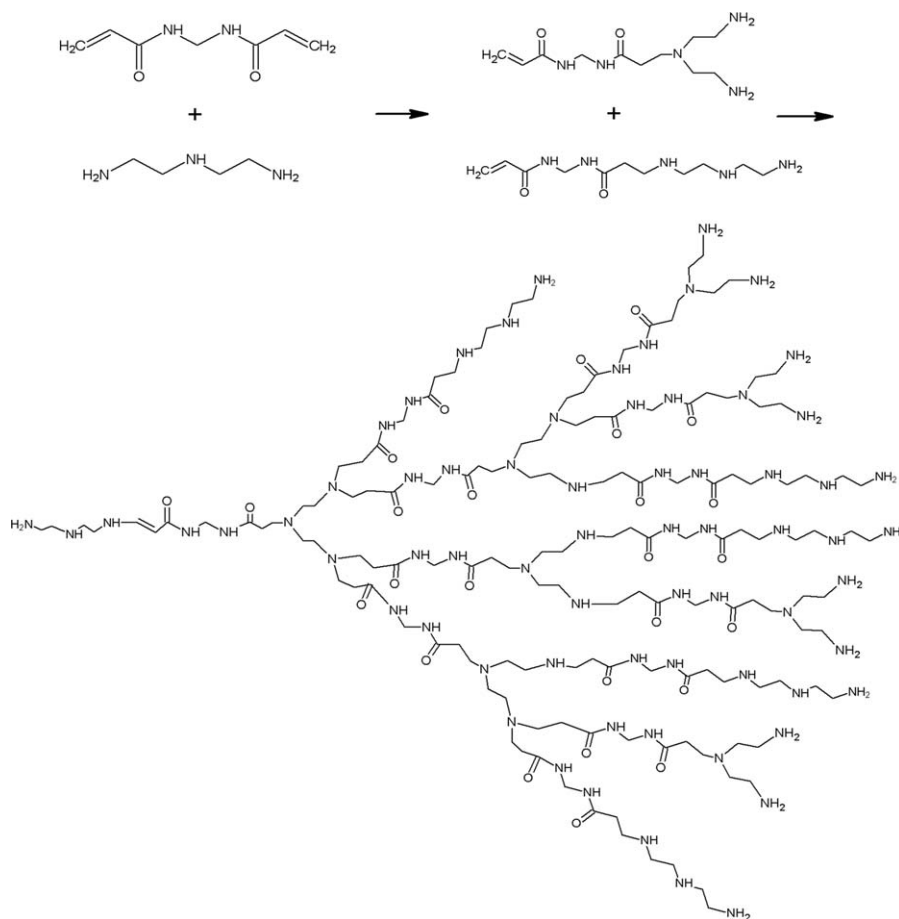
Scheme 1. The synthesis route of HBP-NH$_2$.

(MBA), and diethylenetriamine (DETA) were all provided by Tianjin Fuchen Chemical Regents Factory (Tianjin, China). 6306B Polyurethane was purchased from Yantai huada chemical industry co., LTD (Yantai, China). SF400 Scattered frosted installations was supplied by Changzhou self-reliance chemical machinery co., LTD (Changzhou, China). 101-1AB draught drying cabinet was provided by Talsite instrument co., LTD. (Tianjin, China).

Synthesis of HBP-NH$_2$

According to the methods in previous article,[17] HBP-NH$_2$ had been prepared. A total of 15.417 g MBA was put in a three-necked bottle equipped with a thermometer and condenser, and 11.348 g DETA was weighed and diluted by DMF. Then, diluted DETA was added to above-mentioned three-necked bottle. Then, the mixtures were allowed to react for 24 h at 80°C after stirring and dissolution. Finally, greenish yellow viscous products were obtained. To remove the unreacted monomers, preliminary product was introduced into a pear-shaped funnel, and then acetone whose volume was five times of the product was added to purify the product for three times. Finally, viscous products were produced after the acetone was removed by using rotary evaporator (the vacuum was −0.09 MPa), which was rotated for 30 min at 50°C. Scheme 1 showed the synthesis route of HBP-NH$_2$.

Preparation of Blend Films

The casting solution was prepared by mixing 40 g PU solution(30%) and 3% HBP-NH$_2$ (basing on the weight of dry as PU), and dissolving them with DMF under stirring to achieve a final total solid concentration of 18% (w/w). The mixtures were deaerated in vacuum to remove bubbles, cast onto a clean, dry glass mould, natural flowing, and then dried in a draught drying cabinet at 120°C for 2 h. The PU/HBP-NH$_2$ films were obtained. Scheme 2 showed the reaction mechanism of PU/HBP-NH$_2$ film.

Characterization and Measurements

The rate of moisture absorption of film was measured at room temperature. It was calculated according to dry weight (W_d) and wet weight (W_w) of the film using the following equation:
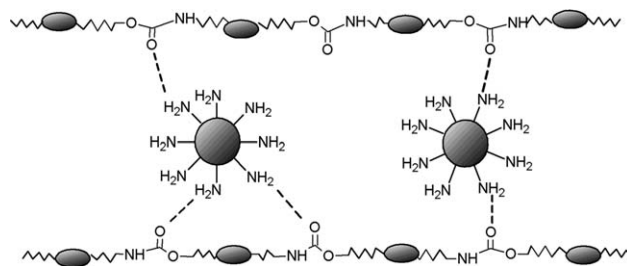
Scheme 2. The reaction mechanism of PU/HBP-NH$_2$ film.

$$W_{ma} = \frac{W_w - W_d}{W_d}$$

where W_d was the weight of film which was dried in oven at 50°C for 24 h and W_w was the weight of film which was soaked in deionized water for 24 h.

The water vapor permeability (WVP) was measured according to the static method. First, 30 mL deionized water was added into a WVP cup, second, the film was fixed on the top of the cup and then it was weighed quickly (m_1). The cup was subsequently placed in a dryer which was filled by some concentrated sulfuric acid and in the constant temperature and humidity chamber. (temperature: 37°C; humidity: 90% RH). Finally, after 24 h the vapor permeability cup was taken out and weighted as m_2. The WVP of films, which is expressed in units of gm^{-2} d^{-1}, was calculated using the following equation:

$$WVP = \frac{m_1 - m_2}{A \times t}$$

where A is the test area of the sample, t is the test time of the sample.

Tensile Tester (PT-1171, Taiwan Baoda International co., LTD, China) was used to measure tensile strength and elongation at break. The test was conducted with extending speed of 100 mm min^{-1} and the dumb-bell shaped specimens were prepared according to GB1040-79. The average value was calculated after each specimen was tested for three times.

Scanning electron microscope (SEM) (TM-1000 SEM, HITACHI Company, Japan) was used to examine the surface of films and cross section. The sample was subjected to brittle fracture in liquid nitrogen. All samples were pasted on objective table using conductive paste then coated with a layer of gold. Finally, the samples were scanned with an accelerating beam voltage of 1.00 kV.

Fourier transform infrared spectroscopy (VECTOR-22, BRUKER Company, Germany) was used to record the FTIR spectra of the films by KBr compression method, using Attenuated Total Reflectance mode (ATR). Each spectrum resulted from 16 scans in the wave number range 400–5000 cm^{-1}. Signal averages were obtained at resolution ratio of 2 cm^{-1}.

Differential scanning calorimetry (DSC) analysis: 5–10 mg samples were weighed for analyzing the thermal stability of the films by thermogravimetric analyses (DSC200PC, Netzsch Company, Germany). Samples were placed in the balance system and heated from 100 to 200°C at a heating rate of 10°C min^{-1} in nitrogen atmosphere.

Thermo gravimetric analysis analysis: 5–10 mg samples were weighed for analyzing the thermal stability of the films by thermogravimetric analyses (TGA-Q500, TA Company, America). Samples were placed in the balance system and heated from 50 to 600°C at a heating rate of 10°C min^{-1} in nitrogen atmosphere.

X-ray patterns of films were obtained by using diffractometer (D/Max-3c, HITACHI Company, Japan) in the 2θ range 4° to 40° at 4° min^{-1} scan rate, with CuKα radiation of wavelength 0.1542 nm.
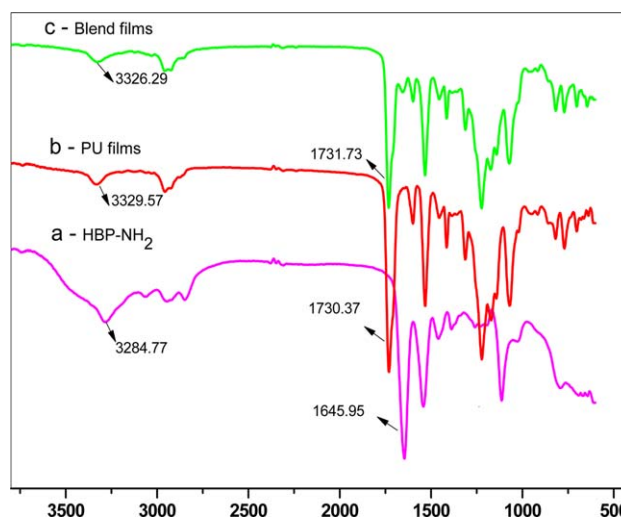
Figure 1. IR spectra of HBP-NH$_2$, PU film, and PU/HBP-NH$_2$ blend film. [Color figure can be viewed in the online issue, which is available at wileyonlinelibrary.com.]

Atomic Force Microscopy (SPM3800-SPA-400, SEIKO Company, Japan) was used to record the surface topography and phase separation morphology of the films. The films were deposited on mica substrates, and the images were obtained in the tapping mode, employing a scan rate of 1.0 Hz, and scanned areas of $1.0 \times 1.0 \ \mu m^2$.

RESULTS AND DISCUSSION

FTIR Analysis

The infrared spectrum is an useful method to study the hydrogen bonding between polymers, which will make the absorption peaks move to lower wavelength. The stronger the interaction is the more greatly the wavelength changes.[18,19] Figure 1 showed FTIR spectra of HBP-NH$_2$, PU, and PU/HBP-NH$_2$ blend films. The characteristic absorption peaks of N—H appeared at 3200 cm^{-1}−3400 cm^{-1} and 1600 cm^{-1}−1750 cm^{-1} belonged to the stretching vibration peak of C=O, respectively. Basing on the analysis of the structures, as far as the position and intensity of the various peaks of the two different films were concerned, the peak appearing at 3200 cm^{-1}−3400 cm^{-1} showed some changes, they weakened and shifted to a lower wave number as the HBP-NH$_2$ introduced (3329.57 cm^{-1} to 3326.29 cm^{-1}). In addition, the intensity of the peak at 1730 cm^{-1} decreased. It indicated the increase of intermolecular hydrogen bonds between PU and HBP-NH$_2$, and N—H in HBP-NH$_2$ molecules and —NHCOO— was the proton donor, and proton receptor was the C=O in PU and HBP-NH$_2$ molecules, analyzed from the structure. On comparing the spectra of PU film and PU/HBP-NH$_2$ blend film, it has been observed that the characteristic band of each ingredient appears as linear superposition, neither more nor less. Based on the results of FTIR, it can be concluded that PU and HBP-NH$_2$ existed as physical blending, and intermolecular hydrogen-bonding interaction were formed to some extent.

X-ray Diffraction Analysis

As shown in Figure 2, the patterns of HBP-NH$_2$ and PU film displayed a diffuse peak at $2\theta = 21°$, which indicated that there
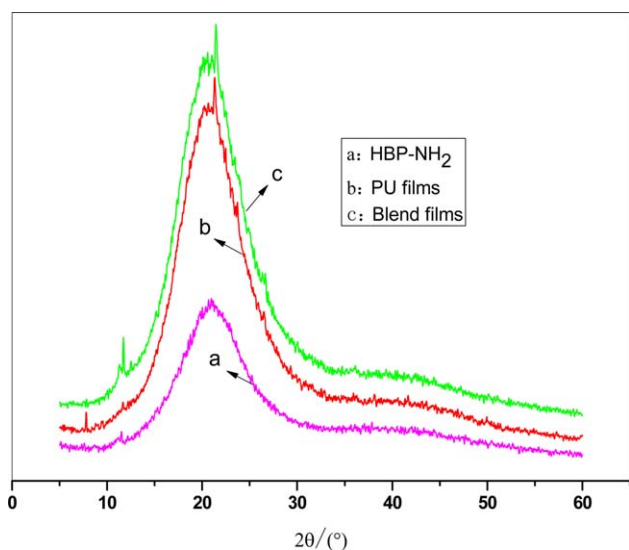
Figure 2. X-ray diffraction patterns of HBP-NH$_2$, PU film, and PU/HBP-NH$_2$ blend film. [Color figure can be viewed in the online issue, which is available at wileyonlinelibrary.com.]
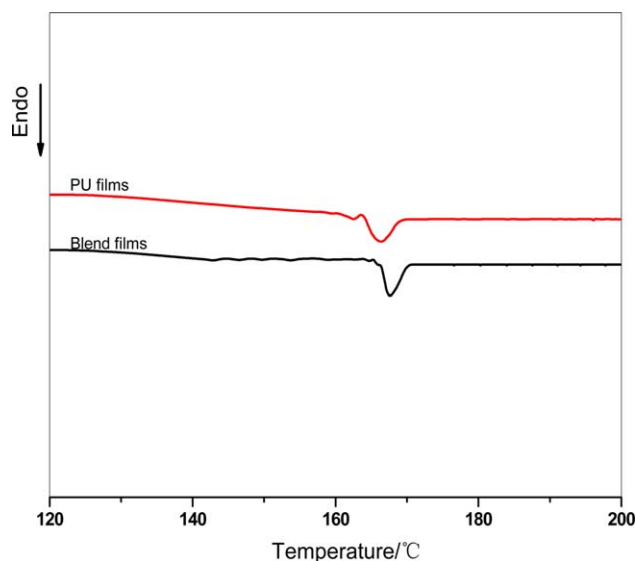

Figure 3. DSC patterns of PU film and PU/HBP-NH$_2$ blend film. [Color figure can be viewed in the online issue, which is available at wileyonline-library.com.]

was crystal structure in PU film. Comparision of PU film and PU/HBP-NH$_2$ blend film showed that the diffraction peak of PU/HBP-NH$_2$ blend film observed at $2\theta = 21°$ became sharp. Meanwhile, a small and weak diffraction peak appeared at $2\theta = 12°$. The results further confirmed that two components in the blend system were easily form intermolecular hydrogen bonding. The research also showed that the interaction between components in blends, such as hydrogen bonding, could reduce the Gibbs free energy of system, so as to make the blending components has good compatibility.[20] It can be expected that HBP-NH$_2$ and PU has good compatibility.

DSC Analysis

DSC is another technique to detect the micro phase separation of the components in the blend by observing the glass transition temperature (T_g). Figure 3 showed the melting temperatures of pure PU and PU/HBP-NH$_2$ blends. There was only one melting peak in the temperature range of measurement, and the increase in melting point was observed when HBP-NH$_2$ was introduced into PU. This phenomenon indicated that the degree of crystallization increased. The increase of intermolecular hydrogen bonds between PU and HBP-NH$_2$ could lead to the decrease of interactions between the soft and hard segments. Then, hard segment was separated from soft matrix, and the regularity of soft segments increased. That is to say, micro phase separation of soft and hard segments in molecular chains was greatly enhanced, and the degree of crystallization increased.

Thermo Gravimetric Analysis (TGA)

In Figure 4(a,b) represented the TG curves of PU film and PU/HBP-NH$_2$ blend film. When temperature was less than 250°C, the weight loss both were within 5%. For the first stage, the weight loss was related to the evaporation of free water. Because there was HBP-NH$_2$ in blend film which had abundant hydrophilic groups, and these groups showed excellent hygroscopicity, the weight loss of blend film was greater than that of PU. The

weight loss in second stage was attributed to the decrosslinking of polymer networks and formation of a carbonaceous residue. The starting thermolysis temperature both was about 450°C. However, the temperature of blend film was higher than that of PU film, and the weight loss of blend film was lower. Moreover, the decomposition rate of blend film was slower, which indicated that the thermal stability of blend film became better. This was because PU and HBP-NH$_2$ had better compatibility, and the degree of crystallization increased.

Morphology Analysis

A series of SEM micrographs were exhibited in Figure 5, which provided the comparison of the two different films. The bottom was the side of films which contacted with the polytetrafluoro-ethylene glass plate. In the film-forming process, the
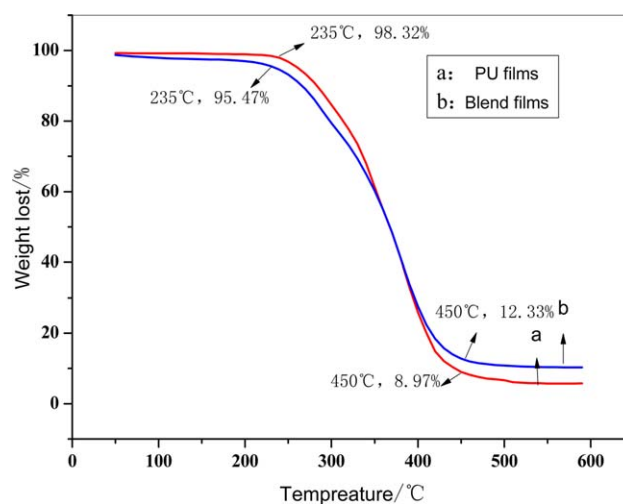
Figure 4. TG patterns of PU film and PU/HBP-NH$_2$ blend film. [Color figure can be viewed in the online issue, which is available at wileyonline-library.com.]
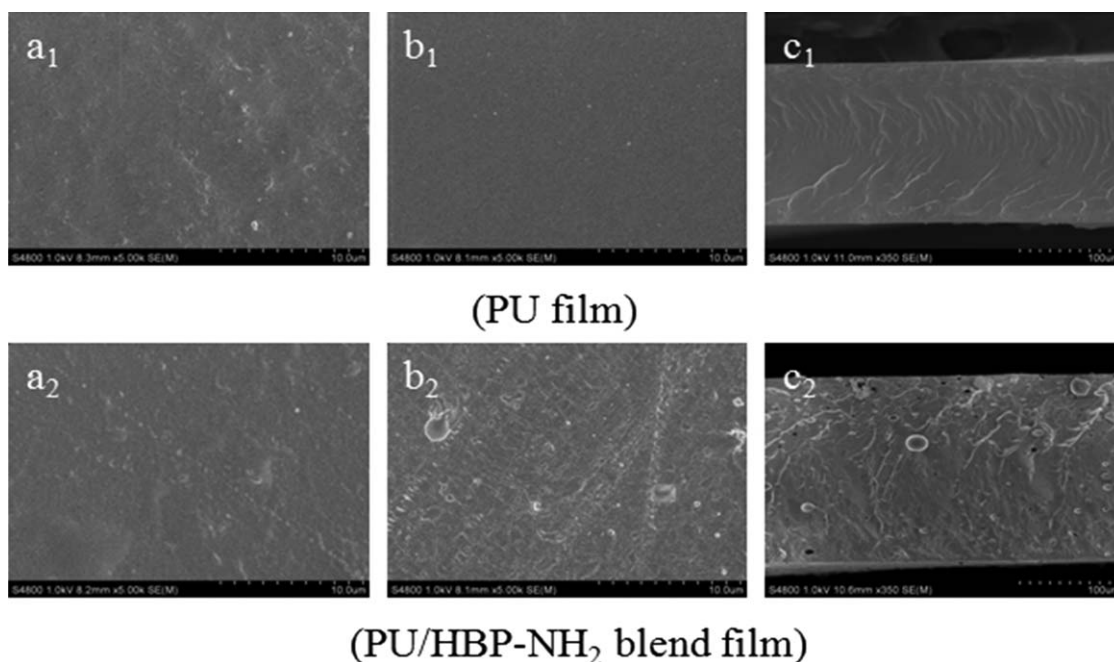
Figure 5. SEM images of PU film and PU/HBP-NH$_2$ blend film (a) the bottom; (b) the surface; (c) the longitudinal section.

evaporation of solvent was so slow that there was no significant difference between two films. Therefore, the bottom of two films was homogeneous. The surface was the side of films that contacted with air. The PU film was formed by homogeneous material, so it was smooth and dense. Whereas in blend film, HBP-NH$_2$ which was as dispersed phase was distributed in PU which was as continuous phase. Because their film-forming rates were different, the surface of blend film was uneven. This observation indicated that a certain degree of phase separation between PU and HBP-NH$_2$ occurred in the blend films. Comparison of the longitudinal section of two films showed that the surface of PU film was compact, smooth, and there was almost no pore, but the blend film appeared some uniform distribution pores, which revealed that, besides a certain degree of phase separation, HBP-NH$_2$ was uniformly distributed in PU owing to their intermolecular hydrogen bonding. The existence of the pores was helpful to improve the air permeability of blend film.

AFM Analysis

It is a suitable technique for height and phase imaging tapping mode AFM across the length scales to investigate the microphase separated structures of PU.[20,21] The AFM phase images and 3D phase images analysis of PU film and HBP-NH$_2$/PU blend film were shown in Figure 6. In the phase images, the films display hard phase domains in a soft matrix. Comparison of AFM images of two films showed that the blend film had relatively nonuniform surface morphology, and its surface roughness was 8.151 nm, whereas that of PU film was 4.966 nm. It could also find that the phase interface between hard and soft phase became clearer. This indicated that in the blends, a certain degree of phase separation between PU and HBP-NH$_2$ occurred. The results were in agreement with that of SEM images.

Test Result of Sanitary and Mechanical Performances of PU Film and HBP-NH$_2$/PU Blend Film

Based on the data in Table I, the rate of moisture absorption and vapor permeability of the blend film was significantly more than that of PU film. The vapor permeating mechanism of PU film was described as follows. The vapor is firstly absorbed by hydrophilic groups via hydrogen bonding. And then under the impetus of the vapor pressure difference on both sides of membrane, the vapor was delivered to another side of the film through small space formed by macromolecular thermal motion. Finally, it was spread to the surrounding environment. The driving force of this diffusion was vapor pressure difference between inside and outside of the film. The reason for this enhancement was that HBP-NH$_2$ molecules with abundant hydrophilic groups were evenly distributed in the blend film, and these active groups could combine with water molecules through hydrogen bonds. Meanwhile, the existence of the evenly distributed pores in the film increased its inner volume, which was to say, the water channels were broadened. Microstructures of film controlled its permeation properties and the diffusion rate of water vapor, and it was more conducive for large number of bigger free volumes available in polymeric membrane to increase the vapor permeability of membrane. In short, the improvement in the hydrophilicity together with the increase in porosity of the film enhanced its sanitary property. The vapor permeating mechanism of PU film and HBP-NH$_2$/PU blend film were showed in Figure 7.

The breaking strength and elongation at break of the blend film both decreased, but the reduction value was not much. This can be explained by the fact that HBP-NH$_2$ had an interaction with PU, which hindered the formation of the hydrogen bonding between the soft and hard segments. Furthermore, the small
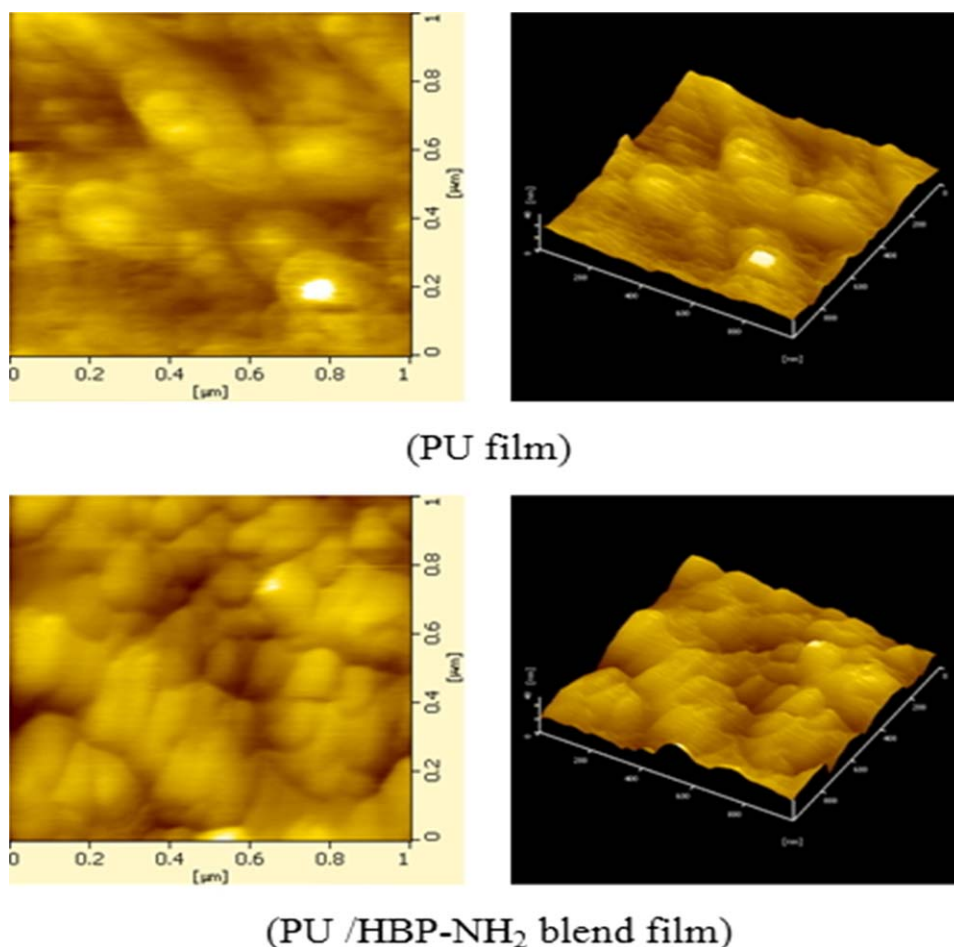
Figure 6. AFM images of PU film and PU/HBP-NH$_2$ blend film (a) phase images (b) 3D phase images. [Color figure can be viewed in the online issue, which is available at wileyonlinelibrary.com.]

pores caused by phase separation between HBP-NH$_2$ and polymer chains also reduced the mechanical strength of film. On the other hand, intermolecular hydrogen-bonding interaction could also ensure the decreasing extent was not too high. Therefore, the blend film can still meet its application requirements.

Compared with natural polymer, less dosage of HBP-NH$_2$ could make the sanitary of film significantly be improved, and the decreasing of mechanical performances was not too high. The WVP and moisture absorption was 5.5 times and 22 times as

high as that of pure PU film when 3% HBP-NH$_2$ was added, and the breaking strength and elongation at break just was reduced by 11.22% and 13.09%, respectively. The superfine chitosan powder and PU blend modification were studied by Zuo et al.[14] The WVP increased from 2000 gm^{-2} d^{-1} to 2510 gm^{-2} d^{-1} when 30% superfine chitosan powders were added, whereas the breaking strength and elongation at break of the blend film decreased from 8.19 MPa to 2.55 MPa and 385% to 300%. In another study,[13] the WVP value of PU/superfine down powder

Table I. Sanitary and Mechanical Performance of PU Film and HBP-NH$_2$/PU Blend Film

Sample	Moisture absorption (%)	Moisture permeability (gm^{-2} d^{-1})	Breaking strength (MPa)	Breaking elongation (%)
PU film	0.34	161	50.6	353.04
PU/HBP-NH$_2$ film (0.1%)	1.72	627.21	49.56	342.21
PU/HBP-NH$_2$ film (0.2%)	5.06	751.42	48.80	326.56
PU/HBP-NH$_2$ film (0.3%)	7.47	879.00	44.92	306.83
PU/HBP-NH$_2$ film (0.4%)	8.31	934.13	44.43	307.21
PU/HBP-NH$_2$ film (0.5%)	8.2	1065.11	44.1	305.76

Remarks: 0.1%, 0.2%, 0.3%, 0.4%, 0.5% was the dosage of HBP-NH$_2$, respectively.
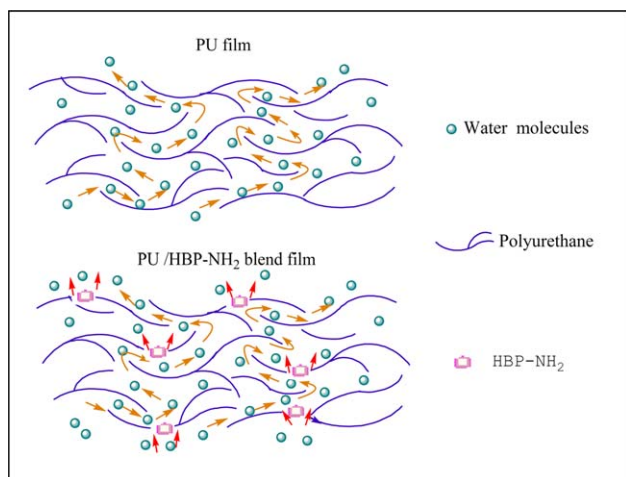
Figure 7. The vapor permeating mechanism of PU film and HBP-NH$_2$/PU blend film. [Color figure can be viewed in the online issue, which is available at wileyonlinelibrary.com.]

composite membranes containing 30 wt % SDP was 14 times as high as that of pure PU membrane, but the breaking strength decreased from 7.334 MPa to 0.943 MPa.

CONCLUSIONS

In summary, PU/HBP-NH$_2$ blend film was prepared by mixing HBP-NH$_2$ solution and PU. Based on the results of IR and XRD, it can be concluded that each component existed as physical blending, and intermolecular hydrogen-bonding interaction were formed to some extent. TG analysis indicated that the blend film with higher thermal stability was obtained, because of the introduction of HBP-NH$_2$. SEM micrographs showed that the blend film appeared some uniformly distributional pores, which indicated that phase separation between PU and HBP-NH$_2$ occurred in the blend films. The rate of moisture absorption and vapor permeability of the blend film significantly increased compared with that of PU film. The breaking strength and elongation at break both decreased a little. The blend film can still meet its application requirements (the breaking strength $>$ 35MPa and the elongation at break $>$ 300%).[22]

ACKNOWLEDGMENTS

REFERENCES

1. Liu, Y. J. Polyurethane Resin and Its Application; Chemical Industry Press: Beijing, **2011**; Chapter 8, pp 315–317.

2. Zhang, W.; Xiao, B.; Zhang, Y.; Yao, H.; Huang, W. L.; Tang, T.; Wang, Y. F. *Chem. Indus. Times* **2007**, *21*, 15.

3. Hong, C. S.; Jikei, M.; Kakimoto, M. *Polym. J.* **2003**, *35*, 859.

4. Wu, J. Y.; Liu, C. H.; Gao, C. *Open Macromol. J.* **2009**, *3*, 12.

5. Yates, C. R.; Hayes, W. *Eur. Polym. J.* **2004**, *40*, 1257.

6. Zhao, L.; Yao, H. Y.; Liu, Y.; Zhang, Y. H.; Jiang, Z. H. *J. Appl. Polym. Sci.* **2013**, *128*, 3405.

7. Xia, Q.; Zhang, M.; Zhao, Y.; Li, L. *Polym. Mater. Sci. Eng.* **2013**, *29*, 60.

8. Kumari, S.; Mishra, A. K.; Krishna, A. V. R.; Raju, K. V. S. N. *Prog. Org. Coat.* **2007**, *60*, 54.

9. Huber, T.; Potschke, P.; Pompe, G. *Macromol. Mater. Eng.* **2000**, *280*, 33.

10. Monticelli, O.; Oliva, D.; Russo, S. *Macromol. Mater. Eng.* **2003**, *288*, 318.

11. Dhevi, D. M.; Prabu, A. A.; Pathak, M. *Polymer* **2014**, *55*, 886.

12. Arfat, Y. A.; Benjakul, S.; Prodpran, T.; Osako, K. *Food Hydrocolloids* **2014**, *39*, 58.

13. Tao, Y.; Yan, Y.; Xu, W.; Zhou, W. *Acta Polym. Sin.* **2010**, *1*, 27.

14. Zuo, D. Y.; Tao, Y. Z.; Chen, Y. B.; Xu, W. L. *Polym. Bull.* **2009**, *62*, 713.

15. Liu, X.; Xu, W.; Li, W.; Chen, Y. *Polym. Eng. Sci.* **2010**, *50*, 2400.

16. Kazuo, H. Patent JP2566799 (B2), **1996**.

17. Ren, L. F.; Zhao, G. H.; Qiang, T. T.; Wang, X. C.; Wang, N. *Text. Res. J.* **2013**, *83*, 381.

18. Bostan, M. S.; Mutlu, E. C.; Kazak, H.; Keskin, S. S. *Carbohydr. Polym.* **2014**, *102*, 993.

19. Zheng, H.; Du, Y. *Acta Polym. Sin.* **2002**, *4*, 525.

20. Tocha, E.; Janik, H.; Dębowski, M.; Vancso, G. *J. Macromol. Sci. Phys.* **2002**, *41B*, 1291.

21. Fernández, C. E.; Bermúdez, M.; Alla, A.; Muñoz-Guerra, S.; Tocha, E.; Vancso, G. *J. Polym.* **2011**, *52*, 1515.

22. Liu, Y. J. Polyurethane Resin and Its Application; Chemical Industry Publishing House: Beijing, **2011**; Chapter 8, pp 320–324.